

# PeriDEM – High-fidelity modeling of granular media consisting of deformable complex-shaped particles

Prashant Kumar Jha <sup>1</sup>

<sup>1</sup> Department of Mechanical Engineering, South Dakota School of Mines and Technology, Rapid City, SD 57701, USA

DOI: [10.xxxxxx/draft](https://doi.org/10.xxxxxx/draft)

## Software

- [Review](#)
- [Repository](#)
- [Archive](#)

Editor: [Open Journals](#)

## Reviewers:

- [@openjournals](#)

Submitted: 01 January 1970

Published: unpublished

## License

Authors of papers retain copyright and release the work under a Creative Commons Attribution 4.0 International License ([CC BY 4.0](#))

## Summary

Modeling dynamics of deforming and breaking particles interacting with each other is a challenging task from both mechanistic modeling and simulation point of views. The PeriDEM library implements a hybrid approach combining peridynamics and the discrete element method (DEM), providing a means to simulate the intricate behaviors of granular systems involving arbitrarily shaped particles and particle breakage. The PeriDEM framework integrates the strengths of DEM, which effectively captures inter-particle contact forces, with peridynamics, which can model intra-particle deformation and fracture. This hybrid approach is particularly suited for scenarios involving extreme conditions such as high-stress environments where particle deformation and breakage play significant roles.

## Statement of Need

Granular materials are prevalent in numerous industrial sectors, including geotechnical, manufacturing, mining engineering, and pharmaceuticals. Current modeling techniques such as DEM struggle with accurately capturing the behavior of granular materials under extreme conditions, especially when dealing with complex geometries and deformable particles. PeriDEM implements a high-fidelity framework combining DEM and peridynamics to allow for accurate simulations of granular systems under extreme loading conditions.

## Background

PeriDEM model was introduced in (Jha et al., 2021), where it demonstrated the ability to model both inter-particle contact and intra-particle fracture for arbitrarily shaped particles. The underlying basic idea is that individual particles are modeled as deformable solid using peridynamics theory, and the contact between two deforming particles are applied at locally at the contact region allowing modeling of complex-shaped particles. The integration of peridynamics within DEM provides a flexible, hybrid framework that handles the contact mechanics at the particle boundary while accounting for the internal material response, including deformation and fracture. This opens up new avenues for exploring the interactions in granular systems, including developing constitutive laws for phenomenological continuum models, understanding effective behavior when subjected to large loading, and impact of particle shape on particle dynamics.

## 35 Brief Introduction to PeriDEM Model

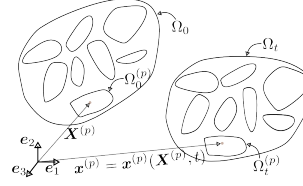


**Figure 1:** Motion of particle system.

36 Suppose a fixed frame of reference and  $\{e_i\}_{i=1}^d$  are orthonormal bases. Consider a collection  
 37 of  $N_P$  particles  $\Omega_0^{(p)}$ ,  $1 \leq p \leq N_P$ , where  $\Omega_0^{(p)} \subset \mathbb{R}^d$  with  $d = 2, 3$  represents the initial  
 38 configuration of particle  $p$ . Suppose  $\Omega_0 \supset \cup_{p=1}^{N_P} \Omega_0^{(p)}$  is the domain containing all particles; see  
 39 [Figure 1](#). The particles in  $\Omega_0$  are dynamically evolving due to external boundary conditions and  
 40 internal interactions; let  $\Omega_t^{(p)}$  denote the configuration of particle  $p$  at time  $t \in (0, t_F]$ , and  
 41  $\Omega_t \supset \cup_{p=1}^{N_P} \Omega_t^{(p)}$  domain containing all particles at that time. The motion  $x^{(p)} = x^{(p)}(X^{(p)}, t)$   
 42 takes point  $X^{(p)} \in \Omega_0^{(p)}$  to  $x^{(p)} \in \Omega_t^{(p)}$ , and collectively, the motion is given by  $x = x(X, t) \in$   
 43  $\Omega_t$  for  $X \in \Omega_0$ . We assume the media is dry and not influenced by factors other than  
 44 mechanical loading (e.g., moisture and temperature are not considered). The configuration of  
 45 particles in  $\Omega_t$  at time  $t$  depends on various factors, such as material and geometrical properties,  
 46 contact mechanism, and external loading. Essentially, there are two types of interactions  
 47 present in the media:

- 48 (1.) *Intra-particle interaction* that models the deformation and internal forces in the particle  
 49 and
- 50 (2.) *Inter-particle interaction* that accounts for the contact between particles and the boundary  
 51 of the domain the particles are contained in.

52 In DEM, the first interaction is ignored, assuming particle deformation is insignificant compared  
 53 to the inter-particle interaction. On the other hand, PeriDEM, accounts for both interactions  
 54 and is summarized next.

55 The balance of linear momentum for particle  $p$ ,  $1 \leq p \leq N_P$ , takes the form:

$$\rho^{(p)} \ddot{u}^{(p)}(X, t) = f_{int}^{(p)}(X, t) + f_{ext}^{(p)}(X, t), \quad \forall (X, t) \in \Omega_0^{(p)} \times (0, t_F), \quad (1)$$

56 where  $\rho^{(p)}$ ,  $f_{int}^{(p)}$ , and  $f_{ext}^{(p)}$  are density, and internal and external force densities. The above equa-  
 57 tion is complemented with initial conditions,  $u^{(p)}(X, 0) = u_0^{(p)}(X)$ ,  $\dot{u}^{(p)}(X, 0) = \dot{u}_0^{(p)}(X)$ ,  $X \in$   
 58  $\Omega_0^{(p)}$ .

### 59 Internal force - State-based peridynamics

60 Since all expressions in this paragraph are for a fixed particle  $p$ , we drop the superscript  $p$ ,  
 61 noting that material properties and other quantities can depend on the particle  $p$ . Following  
 62 (Silling et al., 2007) and simplified expression of state-based peridynamics force in (Jha et al.,  
 63 2021), the internal force takes the form, for  $X \in \Omega_0^{(p)}$ ,

$$f_{int}^{(p)}(X, t) = \int_{B_\epsilon(X) \cap \Omega_0^{(p)}} (T_X(Y) - T_Y(X)) \, dY, \quad (2)$$

64 where  $T_X(Y) - T_Y(X)$  is the force on  $X$  due to nonlocal interaction with  $Y$ . Let  $R = |Y - X|$   
 65 be the reference bond length,  $r = |x(Y) - x(X)|$  current bond length,  $s(Y, X) = (r - R)/R$

66 bond strain, then  $T_X(Y)$  is given by Jha et al. (2021)

$$T_X(Y) = h(s)J(R/\epsilon) \left[ R\theta_X \left( \frac{3\kappa}{m_X} - \frac{15G}{3m_X} \right) + (r - R)\frac{15G}{m_X} \right] \frac{x(Y) - x(X)}{|x(Y) - x(X)|}, \quad (3)$$

67 where

$$\begin{aligned} m_X &= \int_{B_\epsilon(X) \cap \Omega_0^{(p)}} R^2 J(R/\epsilon) dY, \\ \theta_X &= h(s) \frac{3}{m_X} \int_{B_\epsilon(X) \cap \Omega_0^{(p)}} (r - R) R J(R/\epsilon) dY, \\ h(s) &= \begin{cases} 1, & \text{if } s < s_0 := \sqrt{\frac{\mathcal{G}_c}{(3G + (3/4)^4[\kappa - 5G/3])\epsilon}}, \\ 0, & \text{otherwise.} \end{cases} \end{aligned} \quad (4)$$

68 In the above,  $J : [0, \infty) \rightarrow \mathbb{R}$  is the influence function,  $\kappa, G, \mathcal{G}_c$  are bulk and shear moduli  
69 and critical energy release rate, respectively. These parameters, including nonlocal length scale  
70  $\epsilon$ , could depend on the particle  $p$ .

#### 71 DEM-inspired contact forces

72 The external force density  $f_{ext}^{(p)}$  is generally expressed as

$$f_{ext}^{(p)} = \rho^{(p)}b + f^{\Omega_0, (p)} + \sum_{q \neq p} f^{(q), (p)}, \quad (5)$$

73 where  $b$  is body force per unit mass,  $f^{\Omega_0, (p)}$  and  $f^{(q), (p)}$  are contact forces due to interaction  
74 between particle  $p$  and container  $\Omega_0$  and neighboring particles  $q$ , respectively. In (?), the  
75 contact between two particles is applied locally where the contact takes place; this is exemplified  
76 in ?? where contact between points  $y$  and  $x$  of two distinct particles  $p$  and  $q$  is activated  
77 when they get sufficiently close. The contact forces are shown using a spring-dashpot-slider  
78 system. To fix the contact forces, consider a point  $X \in \Omega_0^{(p)}$  and let  $R_c^{(q), (p)}$  be the critical  
79 contact radius (points in particles  $p$  and  $q$  interact if the distance is below this critical distance).  
80 Further, define the relative distance between two points  $Y \in \Omega_0^{(q)}$  and  $X \in \Omega^{(p)}$  and normal  
81 and tangential directions as follows:

$$\begin{aligned} \Delta^{(q), (p)}(Y, X) &= |x^{(q)}(Y) - x^{(p)}(X)| - R_c^{(q), (p)}, \\ e_N^{(q), (p)}(Y, X) &= \frac{x^{(q)}(Y) - x^{(p)}(X)}{|x^{(q)}(Y) - x^{(p)}(X)|}, \\ e_T^{(q), (p)}(Y, X) &= [I - e_N^{(q), (p)}(Y, X) \otimes e_N^{(q), (p)}(Y, X)] \frac{\dot{x}^{(q)}(Y) - \dot{x}^{(p)}(X)}{|\dot{x}^{(q)}(Y) - \dot{x}^{(p)}(X)|}. \end{aligned} \quad (6)$$

82 Then the force on particle  $p$  due to contact with particle  $q$  can be written as (Jha et al.,  
83 2021}):

$$f^{(q), (p)}(X, t) = \int_{Y \in \Omega_0^{(q)} \cap B_{R^{(q), (p)}}(X)} (f_N^{(q), (p)}(Y, X) + f_T^{(q), (p)}(Y, X)) dY, \quad (7)$$

84 with normal and tangential forces following Desai et al. (2019) given by

$$f_N^{(q), (p)}(Y, X) = [\kappa_N^{(q), (p)} \Delta^{(q), (p)}(Y, X) - \beta_N^{(q), (p)} \dot{\Delta}^{(q), (p)}(Y, X)], \quad (8)$$

85 if  $\Delta^{(q), (p)}(Y, X) < 0$  else  $f_N^{(q), (p)}(Y, X) = 0$ , and

$$f_T^{(q), (p)}(Y, X) = -\mu_T^{(q), (p)} |f_N^{(q), (p)}(Y, X)| e_T^{(q), (p)}. \quad (9)$$

## Implementation

PeriDEM is implemented as an open-source library available in GitHub; see [PeriDEM](#). The library is designed with an emphasis on scalability and extensibility, supporting high-performance computing (HPC) through multi-threaded implementations using Taskflow for asynchronous computation. For contact modeling, nanoflann library for tree search is used to find the neighboring discretized nodes.

## Features

- Hybrid modeling using peridynamics and DEM for intra-particle and inter-particle interactions.
- Support for arbitrarily shaped particles, allowing for realistic simulation scenarios.
- Future work includes developing an adaptive modeling approach to enhance efficiency without compromising accuracy.
- Open-source implementation with support for HPC environments, leveraging modern multi-threading techniques for scalability.

## Examples

### Key results

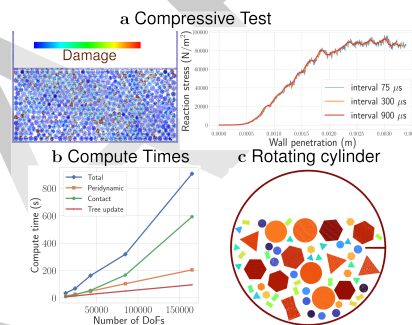


**Figure 2:** Nonlinear response under compression, {b} exponential growth of compute time due to nonlocality of internal and contact forces, and {c} rotating cylinder with nonspherical particles.

The main result from PeriDEM is the compression of 502 circular and hexagon particles in a rectangular container by moving the top wall. The stress on the moving wall as a function of wall penetration becomes increasingly nonlinear, and media shows signs of yielding as the damage becomes extensive; see [Figure 2a](#). Preliminary compute time analysis with an increasing number of particles shows an exponential increase in compute time of contact and peridynamics forces, which is unsurprising as both computations are nonlocal. Demonstration examples also include attrition of various non-circular particles in a rotating cylinder [Figure 2c](#).

## References

- Desai, P. S., Mehta, A., Dougherty, P. S., & Higgs III, C. F. (2019). A rheometry based calibration of a first-order DEM model to generate virtual avatars of metal additive manufacturing (AM) powders. *Powder Technology*, 342, 441–456.
- Jha, P. K., Desai, P. S., Bhattacharya, D., & Lipton, R. (2021). Peridynamics-based discrete element method (PeriDEM) model of granular systems involving breakage of arbitrarily shaped particles. *Journal of the Mechanics and Physics of Solids*, 151, 104376.

- <sup>116</sup> Silling, S. A., Epton, M., Weckner, O., Xu, J., & Askari, E. (2007). Peridynamic states and  
<sup>117</sup> constitutive modeling. *Journal of Elasticity*, 88, 151–184.

DRAFT